

ANALYSIS OF PARTICLE MOTION RECORDED BY THREE-  
COMPONENTS SEISMIC STATIONS

by Mario Ruiz

GEOP 523 FINAL REPORT

December 2003

# ANALYSIS OF PARTICLE MOTION RECORDED BY THREE-COMPONENTS SEISMIC STATIONS

## MOTIVATION

Increasing use of three-component seismometers called attention about some applications of particle motions, which are defined as simultaneous plots of displacements recorded in each component.

A seismic wave field is a superposition of many overlapping wave groups: direct, reflected, refracted, converted, and scattered body and surface waves (Plesinger et al., 1986). At any point on the earth each group has its own shape, velocity, and direction. If the seismic signal is recorded by a seismic station located on the surface or very close to it, the measured particle motion will be influenced by:

- a) the reflection at the free surface (Nuttli, 1961; Nuttli and Whitmore, 1961; Hellweg 2000a; Neuberg and Pointer, 2000),
- b) the effect of the topography (Neuberg and Pointer, 2000), and the anisotropy along the path.

If the signals are recorded by a seismic station located down in a borehole, these effects will decrease.

The orientation of the wave system for each wave group is important information for several applications, such as:

- a) identification of wave type and determination of onset time and pulse duration.
- b) investigation of heterogeneous and anisotropic structures.
- c) epicenter location with a three-component station. Reconstruction of the incident p-wave has been used to find the source location (Del Pezzo et al., 1992, and Neuberg et al., 1994) if the stations are sufficiently close to the source

## FREE\_SURFACE EFFECTS ON PARTICLE MOTION

Free-surface is the strongest discontinuity that intercepts a seismic signal. It is also an important feature because most of seismic stations are located just over the surface or at small depths beneath it.

## CORRECTION BY REFLECTION AT THE FREE SURFACE

Particle motions for P and S plane waves will be analyzed at a horizontal free surface without lateral variations.

First, let's consider an incident P-wave with displacement  $U_{ip}$ , azimuth  $a_0$  and an incident angle  $i$ . The recorded seismic signal which is identified as p-wave is actually the resultant motion

produced by three waves, namely, the incident p-wave, and the reflected p-wave and converted sv wave (Nuttli and Withmore, 1961).

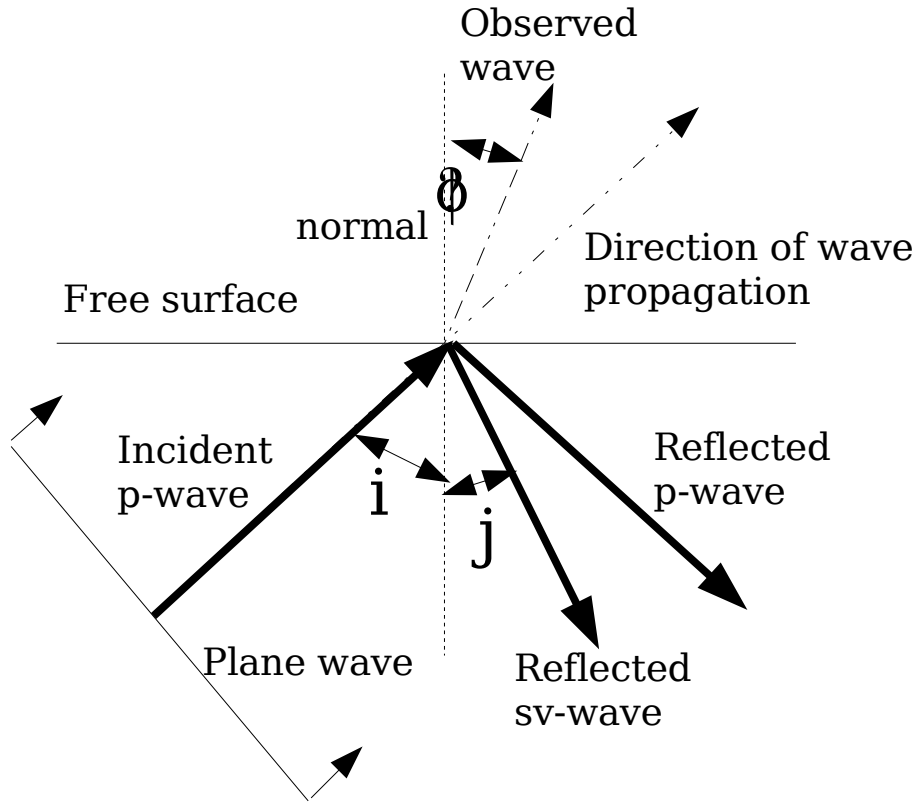


Fig. 1 Incidence angles and particle motion directions for a horizontal free-surface (from Neuberg and Pointer, 2000).

At  $z=0$  (free-surface), shear strains  $\epsilon_{xz}$ ,  $\epsilon_{zz}$ , and tractions will be zero.

For a plane p-wave of amplitude  $P'$ , incident from below, the total displacement  $U$  at the traction-free surface is:

$$U = \frac{\begin{bmatrix} 4\alpha p \cos i \cos j, & 0, & -2\alpha \cos i \left[ \frac{1}{\beta^2} - 2p^2 \right] \end{bmatrix} P' \exp \{i(p x - t)\}}{\begin{bmatrix} \frac{1}{\beta^2} - 2p^2 \end{bmatrix}^2 + p^2 \frac{\cos i \cos j}{\alpha \beta}}$$

where  $\alpha$  and  $\beta$  are the P- and S-wave velocities, respectively, and  $j$  is the emergence angle for Sv reflected wave (Neuberg and Pointer, 2000).  $p$  is the ray parameter:  $p = (\sin i)/\alpha = (\sin j)/\beta$

The apparent p-wave incidence angle  $\Phi$  is defined by the ratio between the horizontal and the vertical components of the displacement:

$$\tan \Phi = \frac{U_{x'}}{U_{z'}} = \frac{\frac{4 \alpha p \cos i \cos j}{\beta^2 \alpha \beta}}{\frac{-2 \alpha \cos i}{\beta^2 \alpha} \left[ \frac{1}{\beta^2} - 2 p^2 \right]} \quad (2)$$

$$\tan \Phi = \frac{2 \sin j \cos j}{1 - 2 \sin^2 j} \quad (3)$$

$$\tan \Phi = \sin 2j / (1 - \sin^2 j - \sin^2 j) \quad (4)$$

$$\tan \Phi = \tan 2j \quad (5)$$

then, we found  $j = \frac{1}{2} \tan^{-1}(\tan \Phi)$

and  $i = \sin^{-1} \left[ \frac{\alpha \sin j}{\beta} \right]$  (6)

Figure 2 shows the differences between the observed “incidence” angle  $\Phi$  and the real incidence  $i$  angle for a  $V_p/V_s = 1.73$ . For angles larger than  $70^\circ$  the residual between these angles becomes larger than 10%, causing significant errors if they are considered the same.

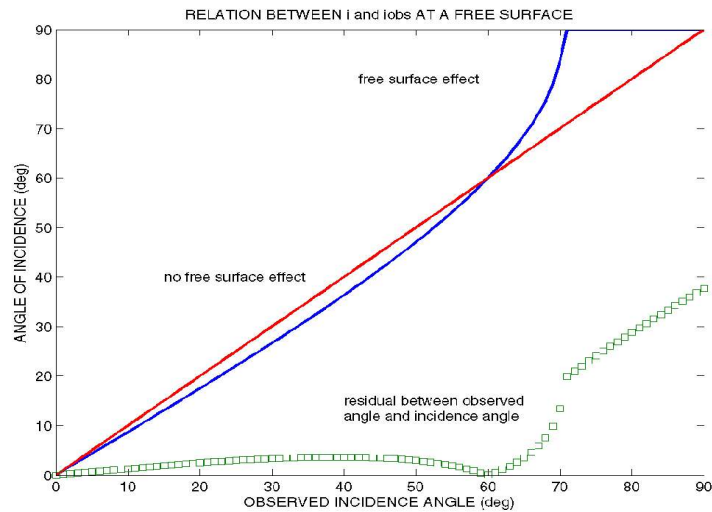


Fig. 2 Relation between angle of incidence of P-wave and the observed incidence angle at the seismograms recorded by a seismic station at the free-surface (blue line) and inside a half space (red line).

If we set  $x=0$ , we may see the amplification caused by the free-surface ( $z=0$ ) effect. In case of an incident x-component of p-wave, the resultant displacement will be:

$$(\sin i + \frac{[\frac{1-2p^2}{\beta^2}] \frac{\alpha}{\beta} + [4\frac{\alpha p \cos i}{\beta} \frac{1-2p^2}{\alpha}]}{[\frac{1-2p^2}{\beta^2}] + 4\frac{p^2 \cos i}{\alpha}}) \sin i + \frac{[4\frac{\alpha p \cos i}{\beta} \frac{1-2p^2}{\alpha}]}{[\frac{1-2p^2}{\beta^2}] + 4\frac{p^2 \cos i}{\alpha}} \cos j$$

Plotting x and z components of p-wave for different times, and setting  $x=0$ , and  $z=0$ , we may construct the particle motion of p-wave in the propagation plane.

In a compact form of the displacement amplitude coefficients can be found using Eq. (95) and Eq. (97) of Geop523 course:

$$u_{pi} = \frac{u_{pr}}{R_p} = \frac{4 r_\alpha r_\beta + (1 - r_\beta^2)^2}{4 r_\alpha r_\beta - (1 - r_\beta^2)^2} \quad (7)$$

with  $r_\alpha = \cot i$   
 $r_\beta = \cot j$

$$\text{or } u_{pi} = \frac{\beta}{\alpha R_s} = \frac{4 r_\alpha r_\beta + (1 - r_\beta^2)^2}{\alpha 4 r_\alpha (1 - r_\beta^2)^2} \quad (8)$$

In case of an incident s-wave, the observed motion at the seismogram is the composition of the incident s-wave, and the reflected s and p-waves. Because of this, the motion of the particle on the earth surface at the time of arrival of s-wave will in general not-be transverse to the ray and not be contained in the plane of the incidence (Nuttli, 1961). Particle motions of s-waves will consider in a separate way the incidence of Sh and Sv components. Using potentials for p-incidence, potentials coefficients are determined for S reflected and P reflected.

Incident Sh at a free-surface will generate at the boundary another Sh wave with equal amplitude and phase of the incident Sh. The particle motion of the incidence of the Sh component is:

$$u_{sob} = 2 u_{si} \cos \omega t \quad (9)$$

where  $\omega$  is the angular frequency of the plane harmonic incidence Sh.

The resultant displacement has twice the amplitude of the incident Sh, causing a free-surface amplification (Aster and Bilek, 2003). For reproducing the horizontal components of the incident S wave, we have to take account this effect.

The incident of Sv waves generate a P-reflected and S reflected waves at the free-surface, both lying in the incidence propagation plane. Using potentials for p and s waves and adequate boundary conditions (strains and tractions = 0 at  $z=0$  free-surface), equations for amplitude

reflections coefficients were found. We have to notice that for incidence angles larger than the critical angle (in case of Poisson solid  $\nu=35^\circ$ ) will generate an evanescent p-wave.

The zero-traction boundary condition at a free surface introduces an amplification of 6 db for vertically incident P and S waves for instruments deployed within a small fraction of a wavelength of the surface

### CORRECTION BY EFFECT OF TOPOGRAPHY

Following Neuberg and Pointer (2000) analysis, a surface is characterized by its normal  $\mathbf{n}$  with a 3-D orientation. The direction of the particle motion is given by  $\mathbf{a}=\mathbf{A}/|\mathbf{A}|$ , and the direction of the incident p-wave by  $\mathbf{b}$ . The dot product of  $\mathbf{a}$  and  $\mathbf{b}$  will give the observed incidence angle. And also:

$$i = \cos^{-1} \mathbf{n} \cdot \mathbf{b} \quad (10)$$

$$\Phi = \cos^{-1} \mathbf{n} \cdot \mathbf{a} \quad (11)$$

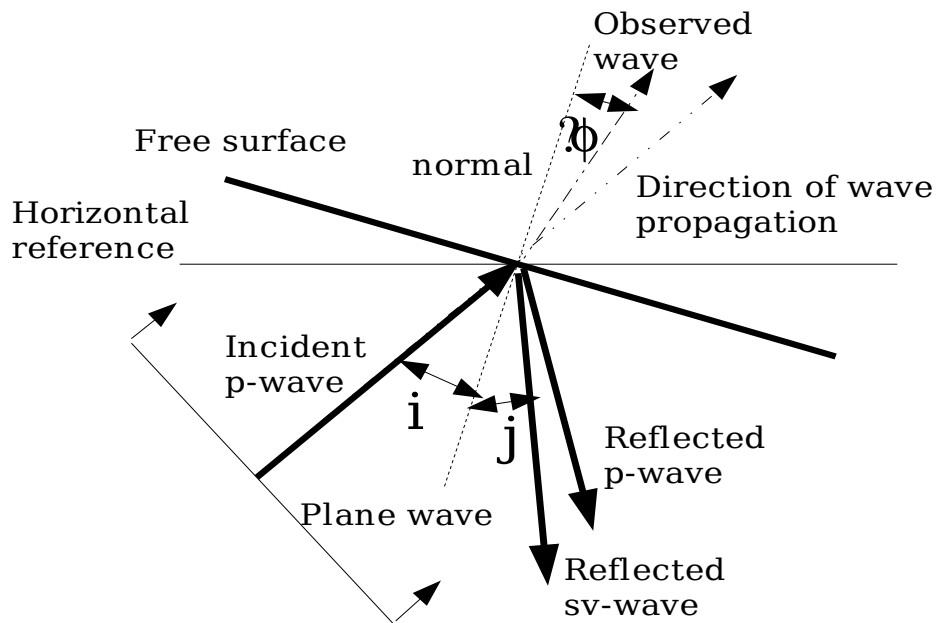


Figure 3. Incidence of a p-wave in a non-horizontal in a non-horizontal free-surface.

### CORRECTION BY EFFECTS OF PATH ANYSOTROPY

In some fields, as volcano seismology, seismic signals are usually affected by the medium along the path, because seismic waves should pass through a highly inhomogeneous medium. Changing the number and location of scatters, Hellweg (2003) studied the influence of the media on the formation of long-duration signals. The polarization at a receiver location for impulsive, sinusoidal or square-wave source when the medium is strongly scattered, mimics the

characteristics of volcanic shocks, tornillos with a single frequency and multichromatic tremor or tornillos (Hellweg, 2003)

## POLARIZATION TECHNIQUE

Polarization analysis makes full use of the 3- component vector field to characterize the particle motion. Most algorithms rely on the eigenvalue analyzes of the data covariance matrix (Schimmel and Gallart, 2003). Generally, polarization analysis of seismic signals is based on Covariance Matrix Method of Matsumara (1981) and Kanasewich (1981). A procedure described below is adapted from Seidl and Hellweg (2003).

- 1) Signal is bandpass-filtered to extract energy around the fundamental frequency and reduce the effect of noise-contamination. The great importance of frequency filtering in studies of polarization properties of waves was pointed out by Plesinger (1985) in his study of the strong ground motions of the Peru Earthquake of Nov. 9, 1974 Generally speaking, lower frequencies carries information of the seismic source and of the medium, meanwhile signal high frequencies may give information about the source process and the local inhomogeneities contained in the medium Vavrycuk (1991).
- 2) The covariance matrix is determined from a selected time window, which should maintain an adequate signal to noise ratio but which should not include multiple signals.
- 3) The X1-X2-X3 coordinate system is determined by the directions of the eigenvalue-eigenvector decomposition of the three-dimensional variance tensor, with X1 and X3 corresponding to the largest and smallest eigenvectors and to the major and minor axes of the polarization ellipsoid, respectively. The eigenvalues are the corresponding energy components and the eigenvectors are the corresponding principal directions. The Z-N-E components are then transformed (rotated) to the X1-X2-X3 coordinate system.
- 4) Considering the orientation of the signal in the X1-X2-X3 coordinate system we may calculate the kinematic parameters: Azimuth  $A_{zn}$  measured clockwise from N, inclination  $I_{nn}$  measured from the vertical, and Rectilinearity is defined as:

$$Re_n = 1 - \left| \lambda_1 / \lambda_2 \right| \quad (12)$$

with  $\lambda_1$  and  $\lambda_2$ , the largest and middle eigenvalues.

## APPLICATIONS OF POLARIZATION

Polarization of P-waves is mostly formed by a simple one-sided pulse followed by secondarily generated waves weaker in some orders of magnitude (Vavrycuk, 1991). P-wave particle motion of a teleseismic event shows the same polarization in the horizontal plane (after introducing a correction by different azimuths of the instruments). SEE FIGURE 03 USGS PEN-FILE REPORT 98-108. The particle motion could be affected by the presence of P'S' waves generated very close to the instrument.

Polarization analysis of P-waves could reveal complexities of the source process. High magnitude double-couple events may have a complex history of the source process (Ruff and Kanamori, 1983; Vavrycuk, 1991).

S-wave content usually is shifted to the lower frequencies. At difference of P-wave polarizations, the polarization pattern of S-waves varies more from one to another, and despite of low frequency content, their polarization pattern looks more complex.

Polarization analysis of S-waves in some regions have two S-waves almost perpendicular in three horizontal projection and follow each other with certain delay. This phenomenon is referred as S-wave splitting, and generally is attributed to the presence of lateral inhomogeneities as oriented crack systems in the Earth's crust, which are responsible for its effective anisotropy.

Kaneshima (1990) found an agreement between the polarization direction of the faster S wave and the direction of the maximum horizontal compressive stress.

Aster et al (1990) found a delay time fluctuation of split S-waves at a maximum of 5-10% in the Anza region in southern California.

Polarization analysis allows to draw some qualitative conclusions about the location of the source of tornillo events ("mostly horizontal polarization for the fundamental modes indicates that the source is near the surface").

## REFERENCES

Aster R.C., Shearer P.M., Berger J., 1990. Quantitative measurements of shear wave polarization at the Anza seismic network, Southern California: Implication for shear wave splitting and earthquake prediction..

Del Pezzo E., Gordano C., Gorini A, and Martini M., 1992. Wave polarization and the location of the source of explosion quakes at Stromboli volcano. In *Volcanic Seismology*, o. 279-296.

Hellweg M., 2000. Physical models for the source of Lascar's harmonic tremor. *J. Volcanol. Geotherm Res.* 101, 138-1

Hellweg M., 2003. The polarization of volcanic seismic signals: medium or source. *J. Volcanol. Geotherm Res.*, 101, 183-198.

Kanasewich E.R. 1981. Time sequences analysis in Geophysics. *J. Geotherm.* The University of Alberta Press,

Matsumura S., 1981. The three dimensional expression of seismic particle motions by the trajectory ellipsoid and its application to the seismic data observed in the Kanto district, Japan. *J. Phys., Earth* 29, 221-239.

Neuberg J. Lockett R., Ripepe R., and Braun T., 1994. Highlights from a seismic broadband array on Stromboli volcano, *Geophys. Res. Lett.*, 21, 749-752.

Neuberg J. and Pointer T., 2000. Effects of volcano topography on seismic broad band of waveforms. *Geophys. J. Int.*, 143, 239-248.

Nuttli O., 1961. The effect of the Earth surface on the S wave particle motion. *Bull Seis. Soc. Am.* 51, 237-246.

Nuttli O. and Whitmore J.D., 1961. An Observational Determination of the variation of the angle of incidence of P-waves with epicentral distance. *BSSA*, 51, N 2, 269-276

Ruff L.J., Kanamori H., 1983. The rupture process and asperity distribution of three great earthquakes from long-period diffracted P-waves. *Physics of the Earth and Planetary Interiors*, 31, 2002, 31, 2002-230.

Schimmel M. and Gallart J., 2003. The use of instantaneous polarization attributes for seismic signal detection and image enhancement. *J. Geophys. Int.*

Seidl D., Helweg M., 2003. Parameterization of multichromatic tremor signals observed at Galeras Volcano (Colombia). *J. Volcanol. Geotherm. Res.*, 125, 171-189.

Vavryuk V., 1991. Polarization properties of Elastic Waves in Anisotropic and Anisotropic media. Ed. Geophysical Institute of Czechoslovak Academy of Sciences. 112 pp.